Research Article GU J Sci 36(4): 1722-1731 (2023) DOI: 10.35378/gujs.1070501

Gazi University

Journal of Science

http://dergipark.gov.tr/gujs

Investigation of Sinterability of WC-Co Component Comprising of AISI 4340 Steel Inserts

Mehmet SUBASI[1,*], Harun KOCAK[2], Asghar SAFARIAN[3], Cetin KARATAS[4]

[1]*Department of Machine and Metal Technology, Technical Sciences Vocational School, Gazi University, Ankara, Türkiye*
[2]*Department of Aircraft Technology, TUSAŞ-Kazan Vocational School, Gazi Universty, Ankara, Türkiye*
[3]*Department of Manufacturing Engineering, Maragheh Branch, Islamic Azad University, Maragheh, Iran*
[4]*Department of Manufacturing Engineering, Faculty of Technology, Gazi University, Ankara, Türkiye*

Highlights

- Parameters were determined for sintering of WC-9% Co feedstock with AISI 4340 steel insert in IPIM.
- Melting occurred at AISI 4340 insert surface during sintering at 1350 °C.
- In the WC-Co part of the samples grain formation started near the intermediate region.

Article Info

Received: 9 Feb 2022
Accepted: 26 Sep 2022

Keywords

WC-Co feedstock
AISI 4340 steel
Sintering
Inserted powder injection molding

Abstract

In this study, sinterability of WC-9% Co component with AISI 4340 steel insert was investigated using Inserted Powder Injection Molding (IPIM) method. Sintering experiments were performed at temperatures of 1200 °C to 1350 °C with dwell times of 120, 240, 360 min. Defects such as gaps, cracks and macro-porosities were observed in specimens, sintered at temperatures of 1200 °C and 1250 °C for all dwell times. It was proved that sintering temperature of 1350 °C was as high as it caused insert to get deformed and melted. As a result, the optimum sintering temperature and dwell time were determined to be 1300 °C and 240 min, respectively, at which the highest hardness, compression strength, and sintered density were obtained without any defects such as cracks or gaps.

1. INTRODUCTION

Powder injection molding (PIM) is a method which has been used for production of metal and ceramic components for nearly fifty years. PIM is a combination of plastic injection molding and conventional powder metallurgy production processes, and is widely used in production of small and complex geometry parts [1,2]. The binder, which shall be removed after injection and in advance of sintering, is used to get injectable feedstock. The binder removal process becomes more difficult in thick components. Therefore, the production of thick and large-sectioned components (thickness > 10 mm) is challenging using PIM. In order to overcome this problem, Inserted Powder Injection Molding (IPIM) method has been developed [3,4]. In IPIM method, a wrought insert is located inside injection mold and then feedstock is injected onto it. IPIM is not only suitable for producing large-sectioned components but also to produce multi-functional components comprising of different materials regarding insert and feedstock [5]. However, sintering behavior of inserted-components consisting of different materials should be considered and investigated because many problems could arise in co-sintering of insert and injected area [6,7]. Guo et al. [8] investigated the production of component consisting of Ti (C, N) -Mo2C-Ni-WC and steel using powder metallurgy. They pointed out that as the thickness of bonding area increased, the defects which were caused because of the component thermal expansion coefficients, decreased. Rodelas et al. [9] combined iron-nickel-tungsten alloy and WC-Co materials with hot pressing and unpressurized sintering techniques. They determined that in non-pressurized sintering, porosities and non-bonded surfaces were formed due to the different shrinkage rates of the materials, while bonding accompanied with less defects by hot pressing. Simchi and Petzoldt [10] investigated the sintering behavior of the parts obtained by co-injection from WC-

*Corresponding author, e-mail: msubasi@gazi.edu.tr

Co and 316L stainless steel feedstocks using Ni interlayer. They specified that the nickel layer formed a liquid film at the interface and therefore the melting temperature of the structure in the intermediate region was reduced.

Sun et al. [11] produced WC-8Co composite components using coarse-grained WC powders in three different sizes. They determined that the dimensions of carbide grains affected the sintering process. They found that the density can be increased as a result of the addition of fine-grained carbide powders into the coarse-grained WC-8Co.

Pötschke et al. [12] mixed different amounts of Co powders with nano-sized WC powders. They sintered the powder mixture at different temperatures between 1150 °C and 1230 °C. They determined that high surface activities of nano sized WC powders had a positive effect on density.

Lan Sun et al. [13] investigated WC grain growth in WC - Co cemented carbide. As a result of the study, they determined sintering temperature and sintering dwell time as the most effective parameters in grain growth.

In the literature, diffusion welding has been used for joining different materials. In this study, sinterability of WC-9% Co feedstock with AISI 4340 steel insert was investigated in IPIM method without applying neither vacuum nor pressure. Firstly, inserts were coated with 100 μm Nickel, after then WC-9% Co feedstock was injected on the inserts. Sintering experiments were performed at temperatures of 1200 °C, 1250 °C, 1300 °C, 1350 °C and sintering dwell times of 120, 240 and 360 minutes. The appropriate sintering temperature and dwell time were determined for both materials, investigating the microstructure and mechanical properties.

2. MATERIALS AND METHODS

2.1. Preparation of The Inserts Coated with Ni

The inner part of the samples consists of AISI 4340 steel inserts and the outer part consists of WC-%9Co feedstock. The feedstock and insert material used in the study were also used in some of our previous studies [14]. Technical properties of the feedstock are given in Table 1. The chemical compositions of the insert material and the feedstock are also given in Table 2. Nickel interlayer with thickness of 100 μm (± 3%) was used as an insert electroplating-coating to improve the quality of the bonding between the insert and the feedstock. Coating conditions are given in Table 3.

***Table 1**. Technical properties of WC-%9Co feedstock*

Powder shape	Density (g/cm^3)	Powder size (μm)		
		D_{10}	D_{50}	D_{90}
Irregular shaped	8.06	0.15	0.28	0.52

***Table 2.** Chemical content of materials*

	C	**Si**	**Mn**	**Cr**	**Mo**	**Ni**	**V**	**W**	**Co**	**P**	**S**	**Fe**
4340	0.39	0.22	0.67	0.78	0.24	1.74	-	-	-	0.025	0.025	Bal..
WC-Co	5.54			0.01	0.01	0.01		Bal..	8.94			0.01

***Table 3**. Electroplating conditions*

Anode	**Bath Temperature**	**Voltage**	**Current density**	**Waiting time**
Electrolytic	50-60 °C	2.5-3 V	4 A/dm²	2 min for 1 μm

2.2. Inserted Powder Injection Molding

The injection process was carried out on the ARBURG Allrounder 220S injection molding machine. Ni coated AISI 4340 inserts were placed into the mold and feedstock was injected then (Figure 1). The parameters used in the injection process are given in Table 4.

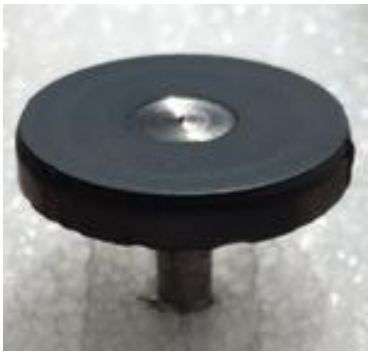

Figure 1. *Sample prepared by IPIM method*

Table 4. *Injection parameters*

Injection Temperature	Injection Pressure	Holding Pressure	Injection Speed	Mold Temperature
200 °C	280 bar	80 bar	10 ccm/s	60 °C

2.3. Debinding and Sintering Process

In the debinding step, the samples were immersed in ethanol at 60 ºC for 48 hours. Then they were subjected to drying in an oven at 60 ºC for 8 hours. Finally, sintering experiments were carried out under atmosphere of 95% N_2 and 5% H_2, at sintering temperatures of 1200, 1250, 1300, 1350 °C, dwell times of 120, 240, 360 minutes, and with heating rate of 5 °C/min.

2.4. Mechanical Tests and Analysis

The density of the sintered samples was determined according to the Archimedes principle. For each sintering dwell time, three different samples (diameter: 4 mm, thickness: 4 mm) were subjected to the compression test according to ASTM E-9 standard, and the average values were reported. Compression tests were performed on an Instron tensile machine with a loading capacity of 50 kN at a constant speed of 1 mm/min. The hardness of the samples was measured by hardness device (HV30). In addition, to evaluate the bonding area in details, image processing tests were also performed using LEICA light microscope, as well as EDS analyzes by JEOL JSM-6060LV Scanning Electron Microscope (SEM).

3. RESULTS AND DISCUSSION

3.1. Effect of Sintering Temperature and Dwell Time on Sintering Behavior

Pötschke et al. [12] stated that hard metals produced by conventional methods are sintered at temperatures higher than 1350 °C. In many studies, it has been seen that the sintering temperature was between 1300-1600 °C and the sintering dwell time was between 60-90 minutes [15,16]. In this study, since it is aimed to sintering of WC-9%Co feedstock with AISI 4340 steel, sintering experiments were performed at lower temperatures compared to the literature. Thus, it has been found that the sintering temperature must be reduced and the sintering time must be increased so that both the insert does not melt and the WC-Co achieves sufficient density and mechanical properties. Therefore WC-Co feedstock was sintered with AISI 4340 insert at temperatures of 1200 ˚C, 1250˚C, 1300˚C and 1350˚C. When the samples were examined

after sintering, it was observed that melting occurred on the insert surface at temperature of 1350 °C (Figure 2a). However, melting problem did not occur at temperatures of 1300 ˚C and lower (Figure 2b).

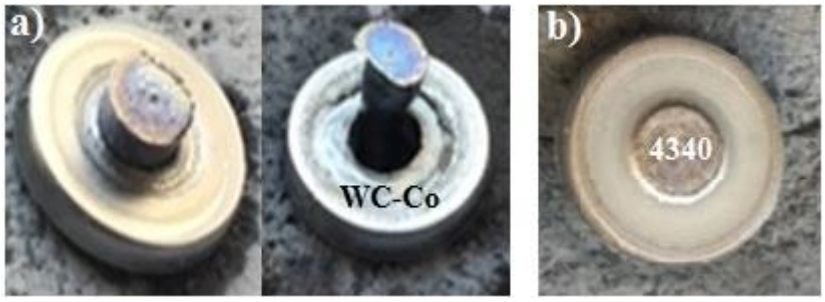

Figure 2. *Sintered samples (a: 1350 °C, b: 1300 °C)*

3.2. Examination of The Injected Section (WC-9% Co) After Sintering

Investigating the SEM images, curvy gaps were observed in sample sintered at temperature of 1200 °C and dwell times of 240 and 360 minutes (Figures 3a and 3b). Sintering the samples at higher temperature of 1250 °C led curvy gaps to be disappeared, however, some macro-porosities were still observed (Figure 3c). Regarding the defects of porosity, the best result was achieved in samples sintered at temperature of 1300 °C, revealing no cracks, no macro-porosities and no gaps (Figure 3d).

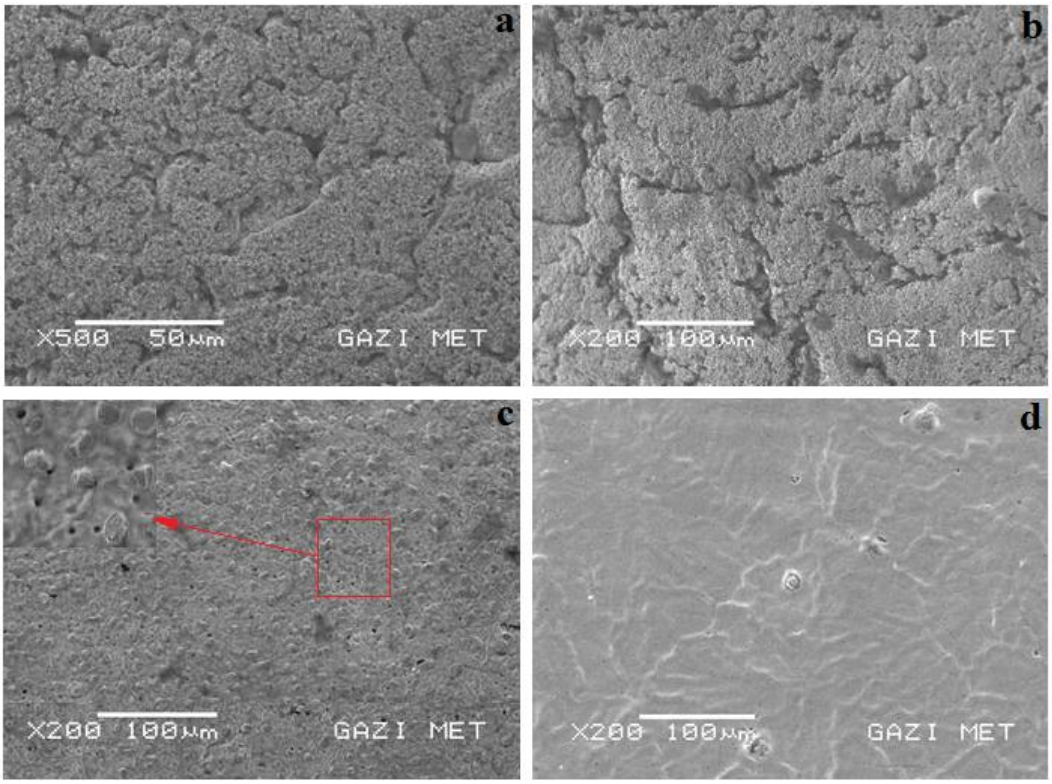

Figure 3. *SEM images of WC-Co after sintering (a: 1200 °C/240 minutes, b: 1200 °C/360 minutes, c: 1250 °C/240 minutes, d: 1300 °C/240 minutes)*

It should also be mentioned that a color change from dark to light gray was determined on the cross-section of WC-Co samples that sintered at 1200 °C for 120 and 240 minutes (Figures 4a and 4b). Although the sintering time increased from 120 minutes to 240 minutes, the color change decreased but did not disappear. However at 1250 °C, the cross-sectional images of the samples became completely light gray.

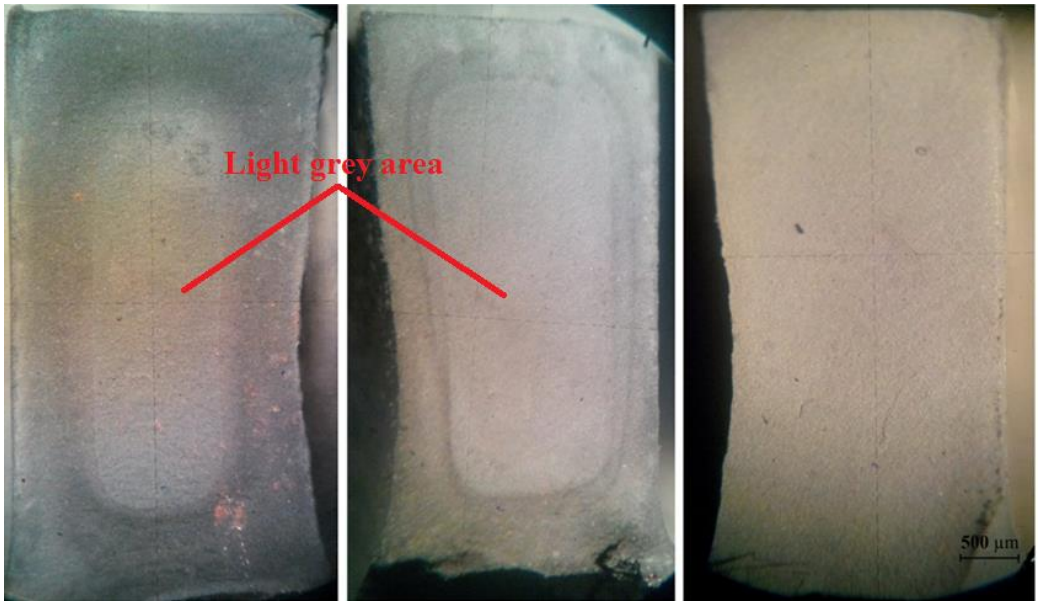

Figure 4. *Cross-sectional view of samples after sintering (a: 1200 ° C 120 min., b: 1200 ° C 240 min., c: 1250 ° C 240 min.)*

It is thought that the color change and the curvy gaps occurred in samples sintered at 1200 °C are caused by the same reason. These problems were arisen because thorough densification cannot be achieved at 1200 °C. German and Bose [17] state that liquid phase formation in sintering WC-Co affects the inter-particle bonding and sample properties. In addition Upadhyaya [18] stated that the liquid phase formation in the WC-Co system starts at approximately 1280 ° C.

It was also reported in the literature that WC dissolution in solid Co powder starts at around 800 °C [19], and formed solid Co solution (0.05-2µm size) becomes saturated up to 1200 °C and solid state shrinkage occurs by Co powders spreading between WC powders [20].

In this study, although the liquid phase formation does not start at 1200 °C, densification of the WC-Co system begins at the interior sections caused by its solid state shrinkage. It can be revealed that the solid state shrinkage in the WC-Co system could lead to an increasing pressure gradient from outside to the inside. Therefore, the densification phenomenon is thought to be occurred from inside to the outside. Comparing the images of Figures 4a and 4b, it can be observed that the densification region in the inside section was increased with increasing the sintering dwell time from 120 minutes to 240 minutes. Observing the SEM images in Figures 3a and 3b, there are some curvy gaps, illustrating this point that the sintering temperature of 1200 °C was not sufficient for sintering, even though there was some densification caused by the solid state shrinkage.

However, both light gray cross-sectional images (Figure 4c) and the disappearance of curvy gaps from the surface in SEM images (Figure 3c) proves that the densification was better in samples sintered at temperature of 1250 °C. But still, the presence of small porosities (Figure 3c) indicated that the sintering temperature should be increased for better sintering. It was seen in Figure 3d that the porosities disappeared due to the liquid phase formation at the temperature of 1300 °C with appropriate sintering compared with temperatures of 1200 °C and 1250 °C.

In this study, it was found that the sintering temperature should be suitable, regarding the thermal properties of the insert, as well as the W-C-Co system in a way to form a liquid phase sintering.

3.3. Microstructure In The Bonding Area

To examine the microstructure of the bonding area, the samples were polished and etched by electrolysis. In Figure 5A, no grain formation was observed, whereas grain formation begins in the region B. The grain formation started from the region-B and the grain size grown up outwards. While the grain size in region B was observed to be around 20 μm, it was between 30 to 68 μm in the region C.

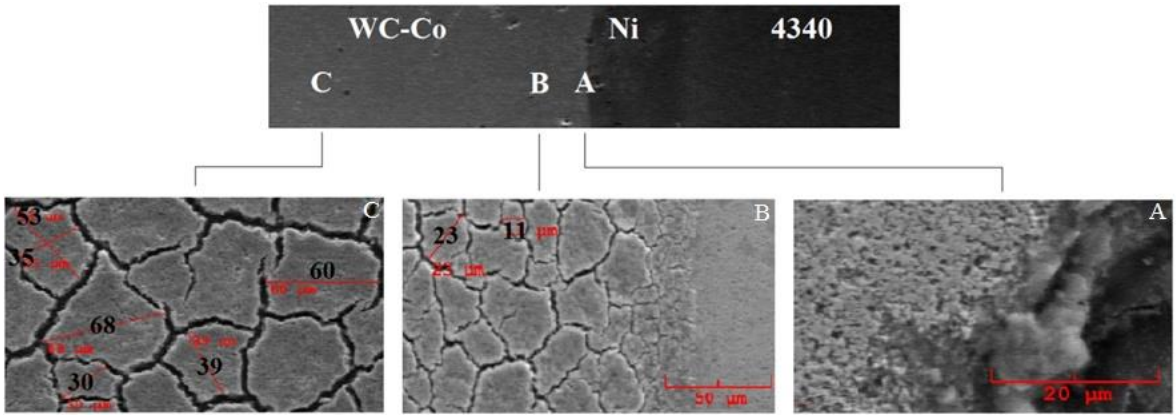

Figure 5. *Microstructure of the bonding area*

It should be discussed that the W and C atoms were separated from the surface of WC powders in the WC-Co system and dissolved in Co. Dissolved atoms spread towards other WC particles, causing the grain growth of WC particles because of recrystallization [21]. Moreover, it has been stated in the literature that carbon ratio is effective in grain growth [22] and grain growth inhibitors such as VC and Cr_2C_3 are used in order to inhibit WC grain growth. Compounds such as VC and Cr_2C_3 dissolve in the Co matrix at low temperatures (1200-1250 ° C) compared with WC, thus it prevents grain growth as W and C dissolution decreases [23].

In this study, nickel is thought to have similar effects on grain growth as inhibitors. In addition, the diffusion of Ni atoms to the WC-Co section, which attach to the surfaces of WC grains, leaded to decrease of carbon (C) dissolution. Thus, grain growth is less due to the low of carbon (C) activity in the sections close to the bonding area. It can be clearly seen in Figure 5 that grain growth occurred from the bonding area towards the outside, in which Ni diffusion was getting lower, accompanied with high C activity.

3.4. Density After Sintering

Samples with a diameter of 10 mm and a thickness of 10 mm were prepared for density measurements. SEM images taken after sintering at 1200 C and 1250 C showed voids and pores. Therefore, no density measurements were made at these temperatures. It was determined that the average density of samples, sintered at 1300 °C for 240 minutes, was 14.04 g/cm^3. In the catalog of the feedstock datasheet of producing company [24] the full density of sintered material has been indicated to be as much as 14.6 g/cm^3. Therefore the maximum density of 96% was achieved in this study.

3.5. Hardness of WC-Co

As a result of the experiments, the highest hardness value was obtained in samples sintered at temperature of 1300 °C and dwell time of 240 minutes. The highest hardness value was reported to be as much as 1679 HV (Figure 6). When the graph given in Figure 6 is examined, it is seen that the hardness of WC-Co increased with increasing sintering temperature and time, which is parallel to the literature [15,25]. It is in the literature that the hardness of the WC-Co material increases as the sintering temperature and time increase. However, in this study, WC-Co material was sintered with a steel insert. Therefore, the sintering temperature should be compatible with both materials. Since the steel insert melted, sintering could not be done at temperatures higher than 1300 °C. As can be seen from the SEM images, increasing the sintering

temperature up to 1300 °C reduces the pores and increases the hardness. However, as the duration time increases, the grain growth also increases. This causes a decrease in hardness [26]. In addition, it is stated in the literature that the hardness of WC-Co for some application s should be in the range of 1500-1900 HV [27]. Compared to the literature, the hardness of the WC-Co material produced in the experiments was found to be sufficient.

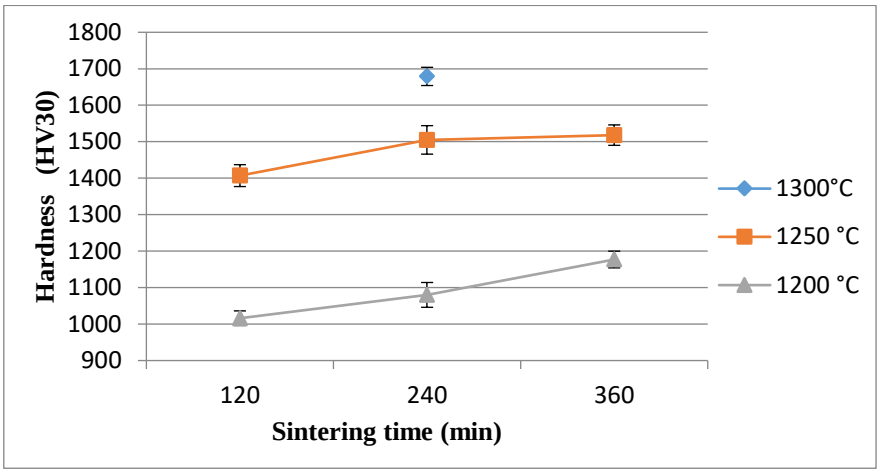

Figure 6. *Effect of sintering temperature and dwell time on hardness of WC-9% Co*

3.6. Compressive Strength

After sintering (three different samples sintered at temperature of 1300 °C) the disk shaped samples were cut with thickness of 4 mm to be subjected to compression tests to evaluate the compression strength of the bonding area (Figure 7). According to these results, the highest compressive strength was obtained at a sintering time of 240 minutes while the lowest compressive strength was obtained at 120 minutes. The compressive strength value decreased with increasing of sintering time from 240 minutes to 360 minutes.

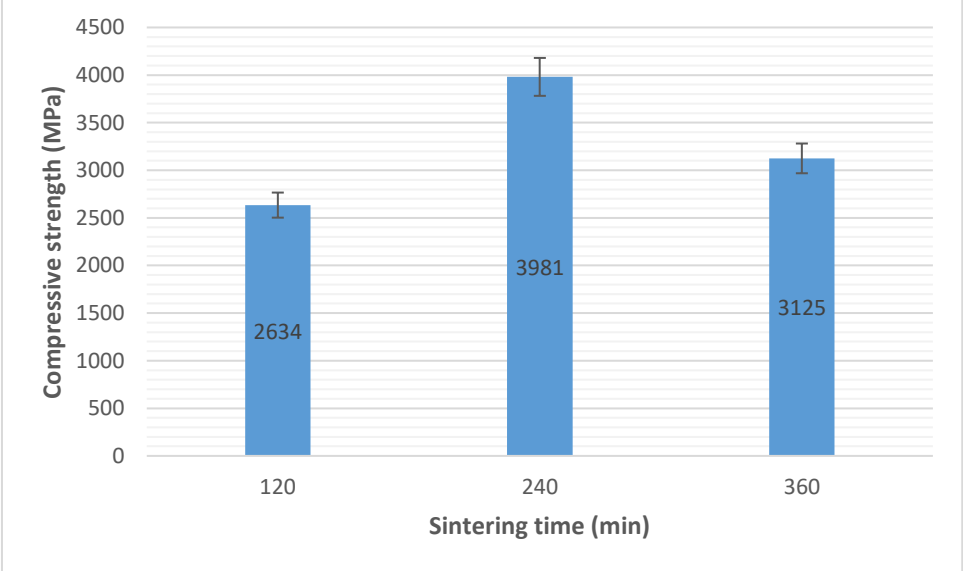

Figure 7. *Effect of sintering time on compressive strength of sample sintered at temperature of 1300 °C*

Okamoto et al. [28] investigated the compressive strength of WC-Co materials having a different percentage of cobalt. They determined that the compression strength decreased with increasing cobalt ratio. In addition, they revealed the compressive strength of samples containing 5%, 10% and 15% cobalt to be 3180, 2810, 2760 MPa, respectively. In another study, Mandel et al. [29] obtained a compressive strength of plasma-sintered WC-12% Co and WC-7% Co, to be 4370 MPa and 6660 MPa, respectively.

In this study, the obtained compressive strength of 3981 MPa, was found to be close to the values in the literature. It was illustrated in the literature that higher compressive strengths could be achieved by increasing the sintering temperature [30], however in our study there was a limitation for applying higher sintering temperatures due to the thermal properties of the AISI 4340 insert material.

4. CONCLUSIONS

In this study, parameters were determined for sintering of WC-9% Co feedstock with AISI 4340 steel insert in IPIM.

- The ideal sintering temperature was determined to be as high as 1300 °C for both of WC-9% Co feedstock and AISI 4340 insert.
- Melting occurred at AISI 4340 insert surface during sintering at temperature of 1350 °C.
- In SEM images, it was found that curvy gaps emerged in samples, sintered at temperature of 1200 °C, which disappeared while sintering at temperature of 1250 °C, still coincident with macro-porosities.
- The macro-porosities disappeared with increasing the sintering temperature of WC-Co to 1300 °C, at which no melting of AISI 4340 insert was reported.
- In sintered samples, grain formation started near to the bonding area at the side of the outer part (WC-Co), with the grain size growing outwards.
- According to the experiments, the highest hardness, compressive strength, and density values were reported in samples sintered at temperature of 1300 °C and dwell time of 240 minutes, to be as high as 1679 HV, 3981 MPa, and 14.04 g/cm^3, respectively.

ACKNOWLEDGEMENT

This research was sponsored by the Scientific and Technological Research Council of Turkey (TUBITAK), Project No: 115M437 and Gazi University Research Funds, Project No: 07/2016-21. The authors would like to express their sincere appreciation to TUBITAK organization and Gazi University for their financial supports.

CONFLICTS OF INTEREST

No conflict of interest was declared by the authors.

REFERENCES

[1] Karataş, Ç., Sarıtaş, S., "Toz enjeksiyonla kalıplama: Bir ileri teknoloji imalat metodu", Journal of the Faculty of Engineering and Architecture of Gazi University, 13(2): 193-228, (1998).

[2] German, R.M., Powder Injection Molding, In ASM Handbook: Powder Metal Technologies and Applications, (1998).

[3] Safarian, A., Subaşi, M., and Karataş, Ç., "Reducing debinding time in thick components fabricated by powder injection molding", International Journal of Materials Research, 106(5): 527-531, (2015).

[4] Safarian, A., Subaşi, M., and Karataş, Ç., "The effect of sintering parameters on diffusion bonding of 316L stainless steel in inserted metal injection molding", The International Journal of Advanced Manufacturing Technology, 89(5): 2165-2173, (2017).

[5] Koçak, H., Samet, K., Yılmaz, O., and Karataş, Ç., "Investigation of composite part production from WC-Co/HSS using nickel interlayer by inserted powder injection molding method", Gazi University Journal of Science Part C : Design and Technology, 6(2): 374-384, (2018).

[6] Johnson, J.L., Tan, L.K., Suri, P., and German, R.M., "Design guidelines for processing bi-material components via powder-injection molding", The Journal of The Minerals, Metals & Materials Society, 55(10): 30-34, (2003).

[7] Heaney, D.F., Suri, P., and German, R.M., "Defect-free sintering of two material powder injection molded components Part I Experimental investigations", Journal of Materials Science, 38(24): 4869-4874, (2003).

[8] Guo, Y., Wang, Y., Gao, B., Shi, Z., and Yuan, Z., "Rapid diffusion bonding of WC-Co cemented carbide to 40Cr steel with Ni interlayer: Effect of surface roughness and interlayer thickness", Ceramics International, 42(15): 16729-16737, (2016).

[9] Rodelas, J., Hilmas, G., and Mishra, R.S., "Sinterbonding cobalt-cemented tungsten carbide to tungsten heavy alloys", International Journal of Refractory Metals and Hard Materials, 27(5): 835-841, (2009).

[10] Simchi, A., Petzoldt, F., "Cosintering of powder injection molding parts made from ultrafine WC-Co and 316L stainless steel powders for fabrication of novel composite structures", Metallurgical and Materials Transactions A, 41(1): 233, (2009).

[11] Sun, Y., Su, W., Yang, H., and Ruan, J., "Effects of WC particle size on sintering behavior and mechanical properties of coarse grained WC–8Co cemented carbides fabricated by unmilled composite powders", Ceramics International, 41 (10): Part B, 14482-14491, (2015).

[12] Pötschke, J., Säuberlich, T., Vornberger, A., and Meese-Marktscheffel, J.A., "Solid state sintered nanoscaled hardmetals and their properties", International Journal of Refractory Metals and Hard Materials, 72, 45-50, (2018).

[13] Sun, L., Jia, C-C., and Xian, M., "A research on the grain growth of WC–Co cemented carbide", International Journal of Refractory Metals and Hard Materials, 25 (2) : 121-124, (2007).

[14] Koçak, H., Subaşı, M., and Karataş, Ç., "Sinter bonding of AISI 4340 and WC-Co using Ni interlayer by inserted powder injection molding", Ceramics International, 45, 22331-22335, (2019).

[15] Heng, S.Y., Muhamad, N., Sulong, A.B., Fayyaz, A., and Amin, M.S., "Effect of sintering temperature on the mechanical and physical properties of WC–10%Co through micro-powder injection molding (μPIM)", Ceramics International, 39 (4) : 4457-4464, (2013).

[16] Eso, O., Fang, Z., and Griffo, A., "Liquid phase sintering of functionally graded WC–Co composites", International Journal of Refractory Metals and Hard Materials, 23(4): 233-241, (2005).

[17] German, R.M., Bose, A., Injection Molding of Metals and Ceramics. First Edition, Metal Powder Industries Federation, New Jersey: Princeton, (1997).

[18] Upadhyaya, G. S., Cemented Tungsten Carbides: Production, Properties, and Testing. Noyes Publications, New Jersey, (1998).

[19] Haglund, S., Ågren, J., "W content in Co binder during sintering of WC–Co", Acta Materialia, 46(8): 2801-2807, (1998).

[20] Allibert, C.H., "Sintering features of cemented carbides WC–Co processed from fine powders", International Journal of Refractory Metals and Hard Materials, 19(1): 53-61, (2001).

[21] Konyashin, I., Hlawatschek, S., Ries, B., Lachmann, F., Dorn, F., Sologubenko, A., and Weirich, T., "On the mechanism of WC coarsening in WC–Co hardmetals with various carbon contents", International Journal of Refractory Metals and Hard Materials, 27(2): 234-243, (2009).

[22] Sugiyama, I., Mizumukai, Y., Taniuchi, T., Okada, K., Shirase, F., Tanase, T., Ikuhara, Y., and Yamamoto, T., "Carbon content dependence of grain growth mode in VC-doped WC–Co hardmetals", International Journal of Refractory Metals and Hard Materials, 52, 245-251, (2015).

[23] Konyashin, I., Ries, B., and Lachmann, F., "Near-nano WC–Co hardmetals: Will they substitute conventional coarse-grained mining grades", International Journal of Refractory Metals and Hard Materials, 28(4): 489-497, (2010).

[24] http://www.ryerinc.com. Access date: 10.06.2019

[25] Erdoğan, M., Erol, A., and Yönetken, A., "Characterization and mechanical properties of WC-Co based scratch", Afyon Kocatepe University Journal of Sciences and Engineering, 13 (025701) : 1-11, (2013).

[26] Fabijanić, T. A., Alar, Ž., and Ćorić, D., "Influence of consolidation process and sintering temperature on microstructure and mechanical properties of near nano-and nano-structured WC-Co cemented carbides, International Journal of Refractory Metals and Hard Materials, 54, 82-89, (2016).

[27] Sarıtaş, S., Türker, M., and Durlu, N., Toz Metalurjisi ve Parçacıklı Malzeme İşlemleri Türk Toz Metalurjisi Deneği, Ankara, (2007).

[28] Okamoto, S., Nakazono, Y., Otsuka, K., Shimoitani, Y., and Takada, J., "Mechanical properties of WC/Co cemented carbide with larger WC grain size", Materials Characterization, 55(4): 281-287, (2005).

[29] Mandel, K., Radajewski, M., and Krüger, L., "Strain-rate dependence of the compressive strength of WC–Co hard metals", Materials Science and Engineering: A, 612, 115-122, (2014).

[30] German, R.M., Liquid Phase Sintering. Springer, Boston, MA, Rensselaer Polytechnic Institute Troy, (1985).